

“Maximizing reversible capacity by suppressing interlayer cation migration in Li-ion electrodes”

Julija Vinckeviciute, Maxwell D. Radin, Nicholas V. Faenza, Glenn G. Amatucci, and Anton Van der Ven

Electronic Supplementary Information

Contents

Experimental data.....	1
O p pDOS.....	1
Exploring Li ordering configurations.....	4
Effect of lattice parameters.....	5
Hubbard U.....	7
TM migration.....	10
Energy cutoff and k-point convergence.....	10
References.....	11

Experimental data

The trend lines in Figure 1(c) are linear fits using least squares regression.

For the $M = \text{Ni}$ linear fit, the equation is irreversible capacity = $11.06 \cdot y + 16.72$ with $R^2 = 0.29$

For the $M = \text{Co}$ linear fit, the equation is irreversible capacity = $120.94 \cdot y + 7.87$ with $R^2 = 0.99$

These lines are largely included as a guide to the eye.

O p pDOS

Figures S1, S2, and S3 contain the overlaid total DOS and the pDOS of O p states in each of the hosts for each dopant, in both D_{oct} and D_{tet} configurations. The unit cells (u.c.) were $4 \times 4 \text{ Li}_x \text{MO}_2$ units (where M is some dopant or transition metal). The energy cutoff for these calculations was 520 eV. The k-point mesh density used was 30 \AA for relaxations and 40 \AA for DOS calculations. DOS have been aligned by the deep O s states (below those pictured) and such that the Fermi level is at 0 eV for the bulk layered material (not pictured). The pDOS labeled “Ox p defect” refer to pDOS associated with the p states of the O atoms that have the lowest amount of charge coordinating them. For instance, in the Li-Al D_{oct} configuration in the Ni host, “Ox p defect” corresponds to the O next to the octahedral Al but not next to any Li atoms. In the Li-Li D_{tet} configuration in the Ni host, “Ox p defect” corresponds to the O next to a single tetrahedral Li and no other Li atoms.

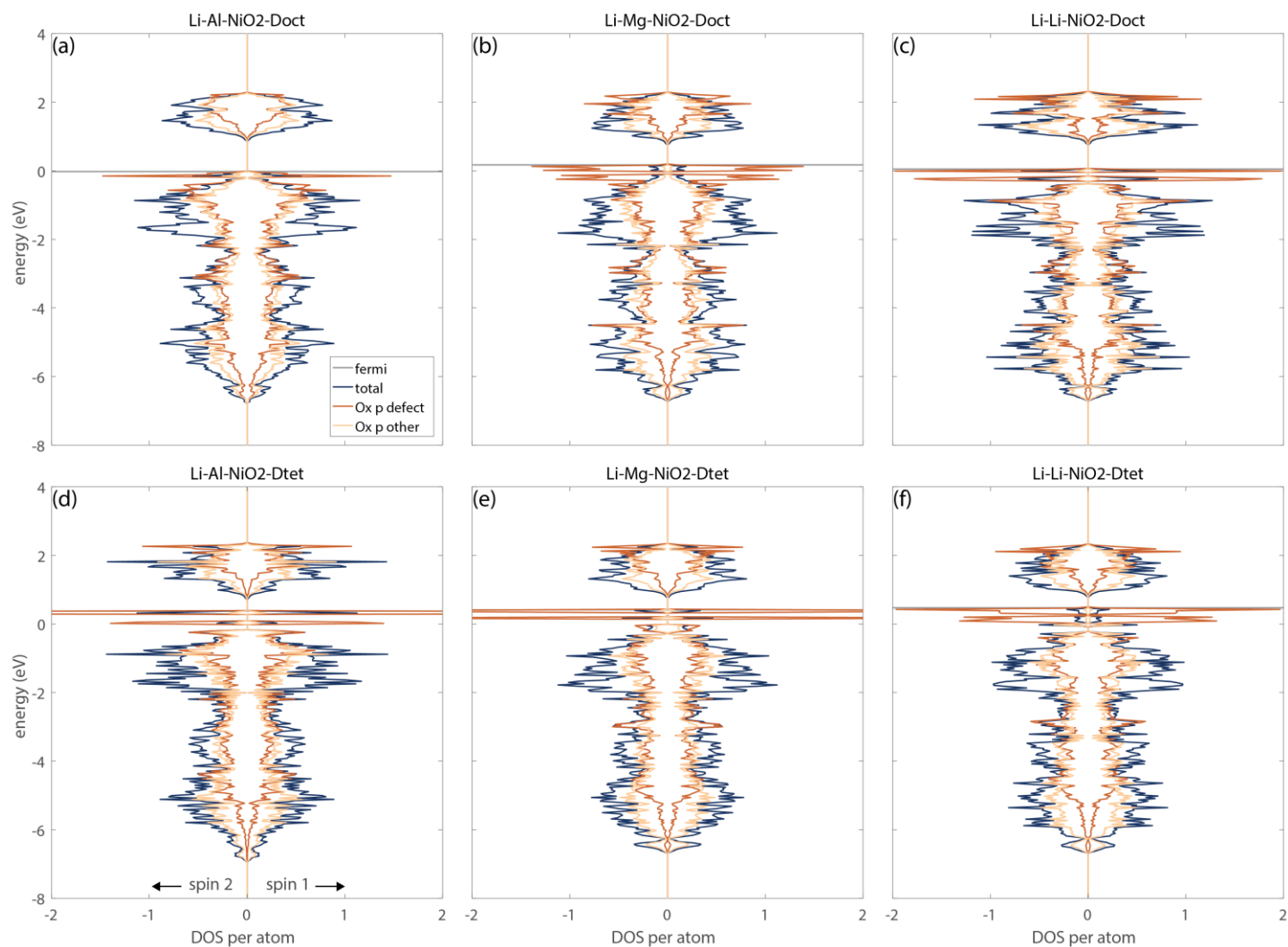


Figure S1. Total and partial DOS for dopants in the Ni host.

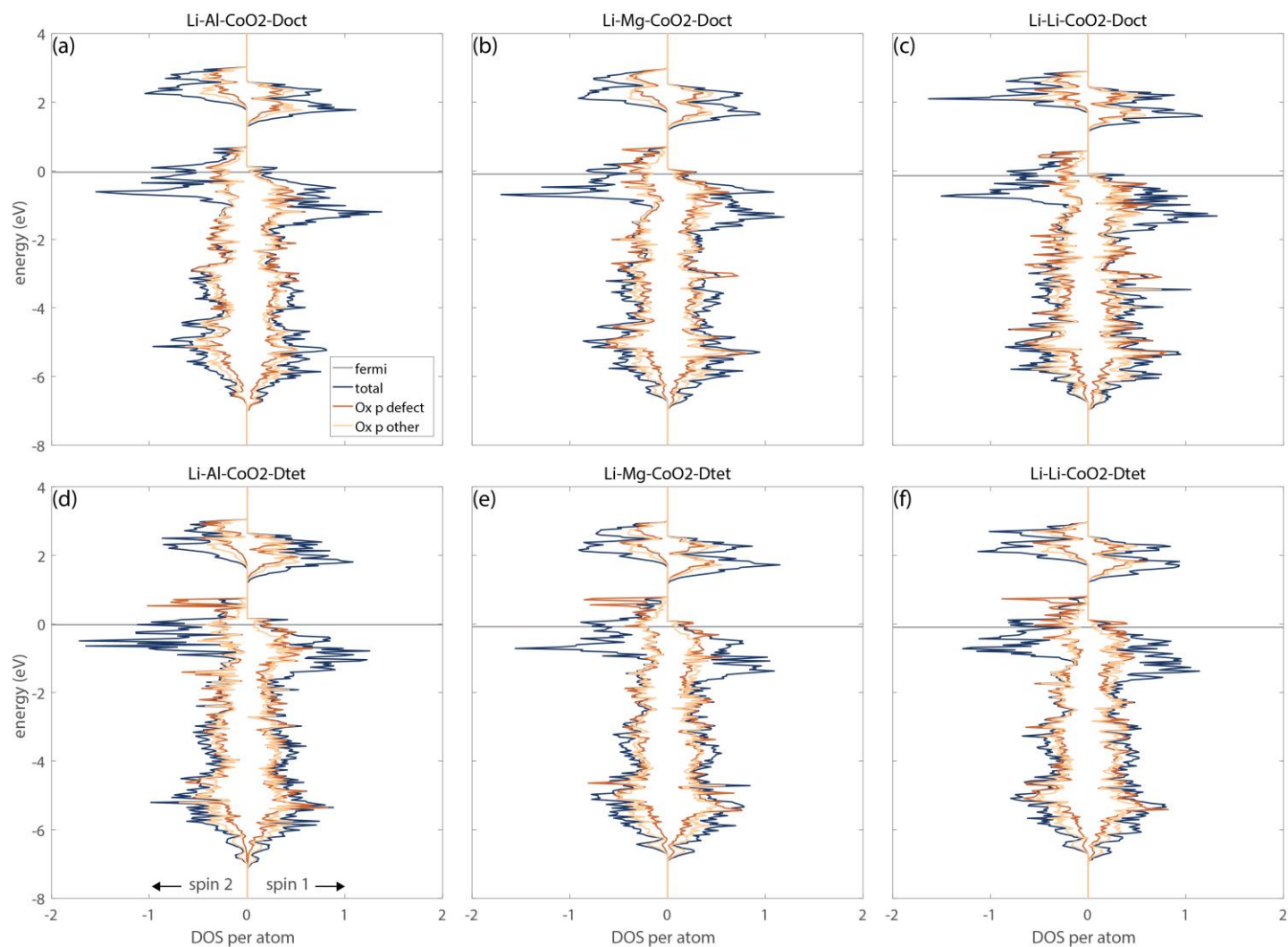


Figure S2. Total and partial DOS for dopants in the Co host.

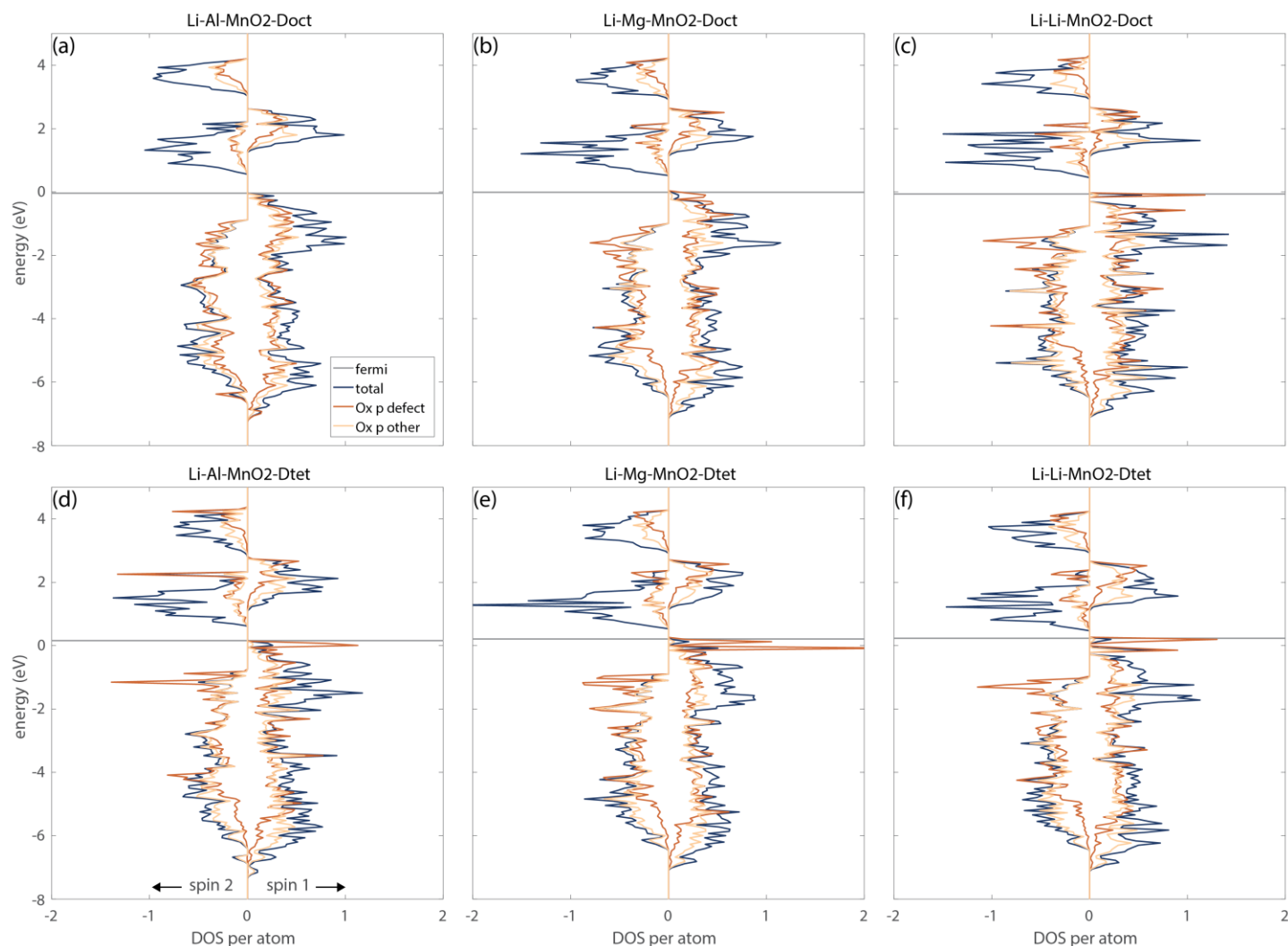


Figure S3. Total and partial DOS for dopants in the Mn host.

Exploring Li ordering configurations

In many configurations that contain extra Li for charge balance, the Li atoms can occupy many different orderings. While exploring the entire configurational space for each dopant-host combination was intractable, we made an extensive effort to determine the lowest energy D_{oct} and D_{tet} configurations. We utilized the CASM software to enumerate the configurations explained below and VASP software to calculate their energies. The k-point mesh density used was 38 \AA and the energy cutoff for these calculations was 530 eV. Files used for calculations are publically available. The energies relative to the lowest energy configuration are shown in Figure S4. While we did not calculate all of the possible configurations, we found that of the ones calculated, the stable configuration was significantly lower in energy than the next lowest configuration, in all cases more than 100 meV per unit cell. That is, in each column of Figure S4, the lowest configuration is set to 0 eV/u.c. and is the one used for our analysis in this work. The configuration with the next lowest energy right above the stable structure is at least 100 meV higher in each column.

For the D_{oct} configurations, the dopant was used to substitute for one of the TM atoms in the TM layer, while the extra Li (1 for Al, 2 for Mg, or 3 for Li) could occupy any of the 16 octahedral sites in the Li layer. For the D_{tet} configurations, the dopant and one of the Li atoms formed a dumbbell, and any leftover Li could occupy octahedral sites in the Li layer that were not face-sharing with the dumbbell. For the Li-Al D_{tet} configuration in Ni and Co hosts, we also calculated

configurations in which the Li in the Li-Al dumbbell was moved to other sites. However, it was found that the dumbbell configuration was the lowest energy configuration.

Of the configurations that were successfully calculated, the lowest energy configurations were those that clustered the extra Li around the defect. The preference of Li to coordinate O around the defect aligns with the findings discussed in this paper since we predict that O surrounded by less charge result in defect states that are higher in energy.

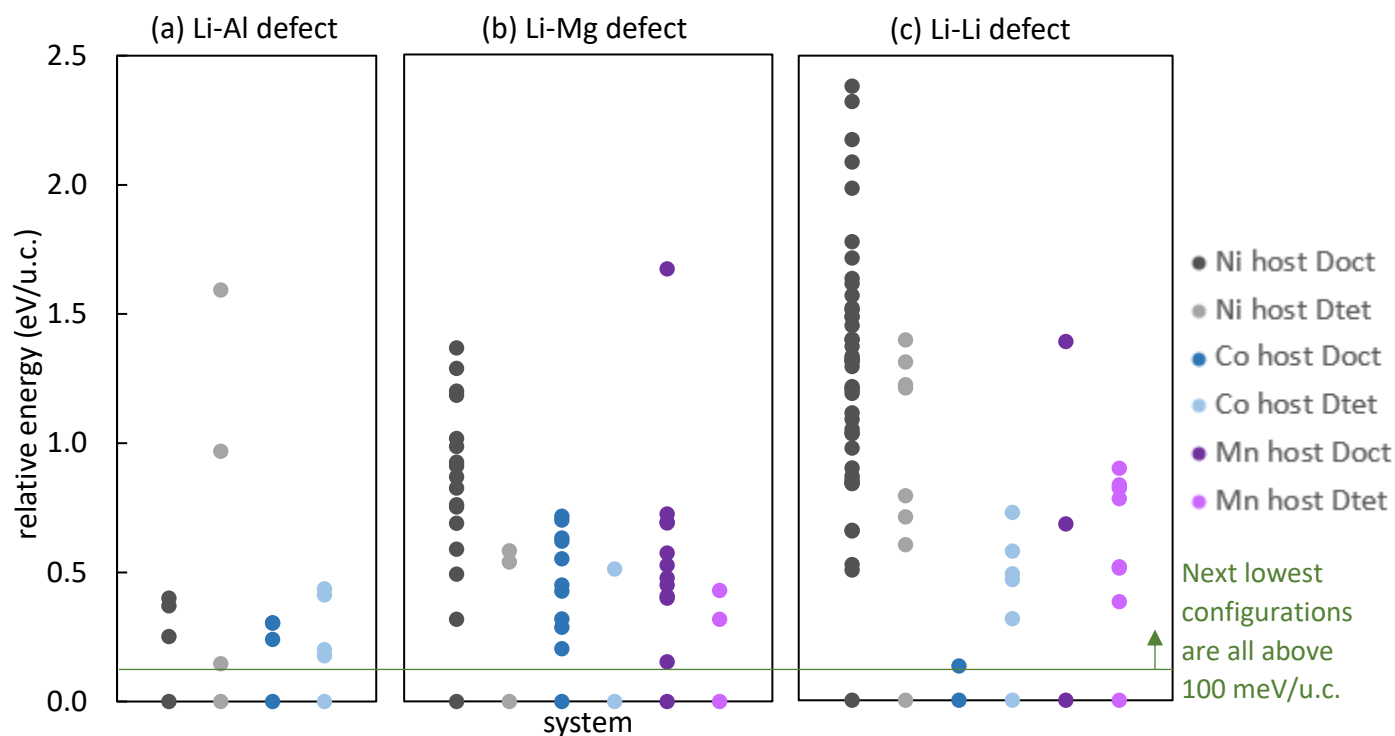


Figure S4. Comparing energies of different Li configurations for D_{oct} and D_{tet} dopant-host systems. Of the configurations calculated, the stable configurations used in the paper were more than 100 meV/u.c. lower in energy than the next lowest configurations.

Effect of lattice parameters

To determine the effect of lattice parameter changes on the energetics and electronic structure, we interchanged the relaxed lattice parameters and atom positions between the different hosts. Static DFT calculations were run using VASP software. The results confirm that lattice parameter differences between the three hosts do not significantly influence stability of D_{oct} versus D_{tet} configurations. The k-point mesh density used was 30 Å and the energy cutoff for these calculations was 520 eV.

D_{oct} and D_{tet} configurations with a Li-Al defects were generated using a 4x4 TM-oxide host. The resulting energy differences between D_{oct} and D_{tet} configurations are shown in Figure S5. The values are grouped by the host that the static calculation was run on. The color indicates which host provided the relaxed structure values. For instance, the purple bar in the “Co host” section is the difference in energy between a static Li-Al D_{oct} configuration in the Co host (using the lattice parameters and atom positions from a relaxed Li-Al D_{oct} configuration in the Mn host) and a static Li-Al D_{tet} configuration in the Co host (using the lattice parameters and atom positions from a relaxed Li-Al D_{tet} configuration in the Mn host). The energy differences vary slightly when the parameters are changed, but do not affect the overall trend (i.e. D_{oct}

configurations are more stable in the Ni host than in the Mn or Co hosts). The total DOS for each calculation are also very similar qualitatively, as shown in Figure S6.

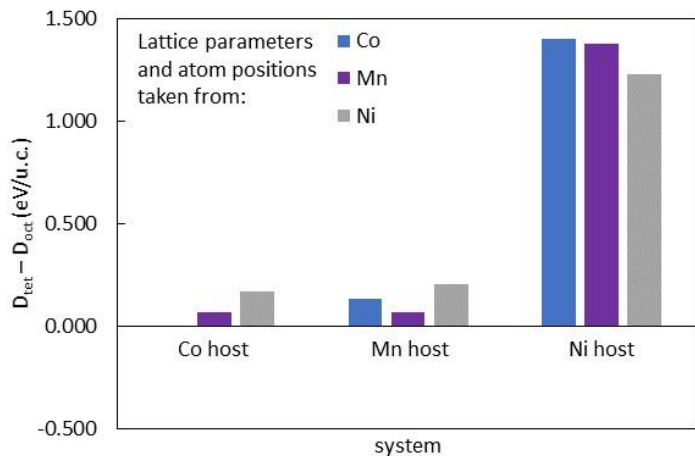


Figure S5. Li-Al dumbbell formation energy for “switched lattice parameter” calculations.

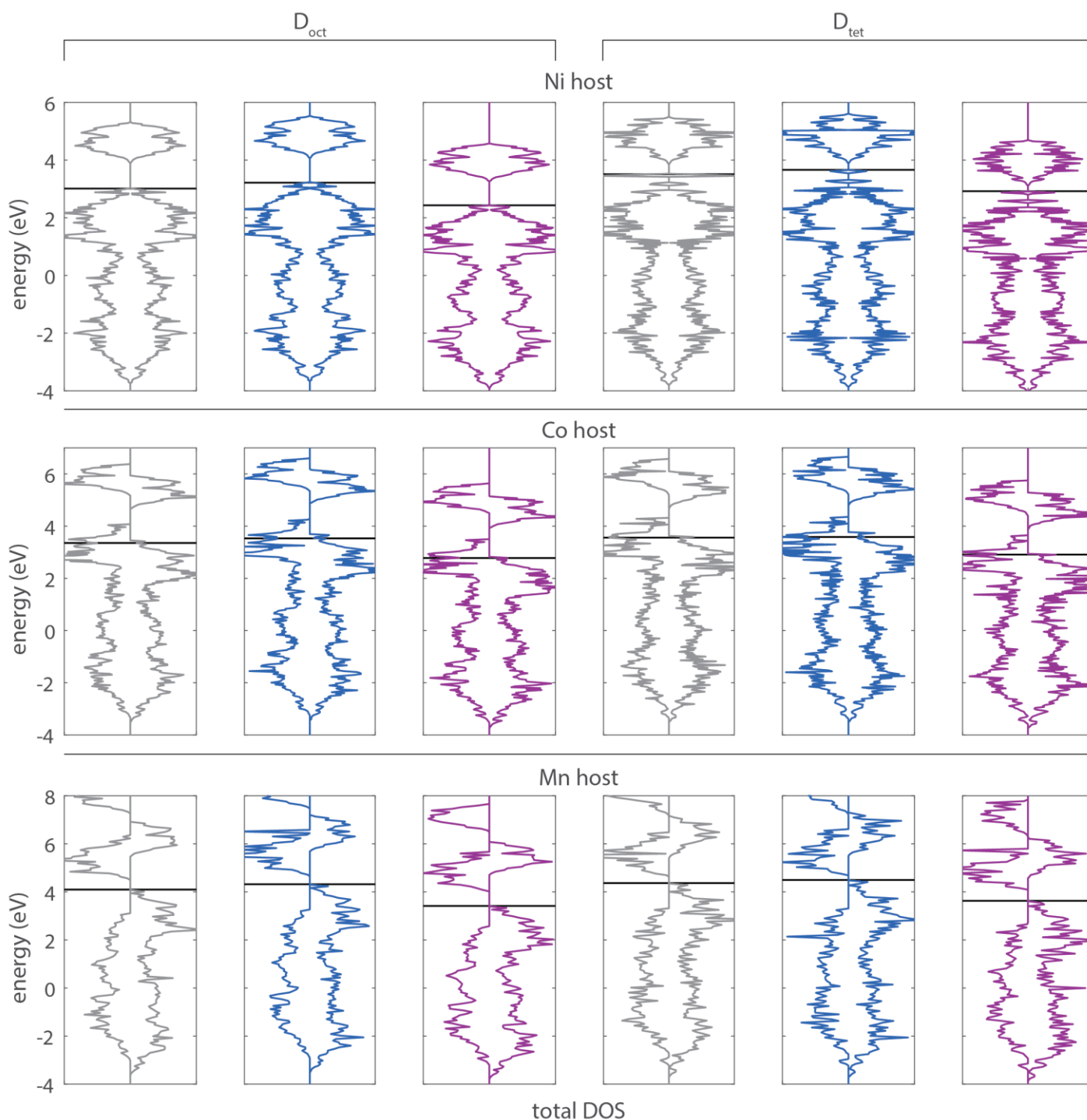


Figure S6. Total DOS for “switched lattice parameter” calculations. Each row has static calculations for the same host (the identity of the TM in the calculation) while the colors indicate which lattice parameters were used (grey – from Ni host, blue – from Co host, purple – from Mn host). The first three columns are for the Li-Al D_{oct} configuration; the last three columns are for the Li-Al D_{tet} configuration.

Hubbard U

All of the calculations reported in the manuscript were done with no Hubbard U correction. Some reports indicate that a Hubbard U correction is important to more accurately model TM-oxide systems. We tested U values of 0, 1, 3, and 5 eV for Li-Al D_{oct} and D_{tet} configurations in Ni and Mn hosts. We did not test addition of the Hubbard U term onto the Co host

because previous studies have shown that the correction results in incorrect charge ordering and ground state configurations^{1,2} in Co oxide systems. The k-point mesh density used was 30 Å and the energy cutoff for these calculations was 520 eV. We allowed lattice parameters and atomic positions to fully relax and calculated the energy difference between D_{oct} and D_{tet} configurations (Figure S7). We also provide total DOS plots for comparison in Figure S8.

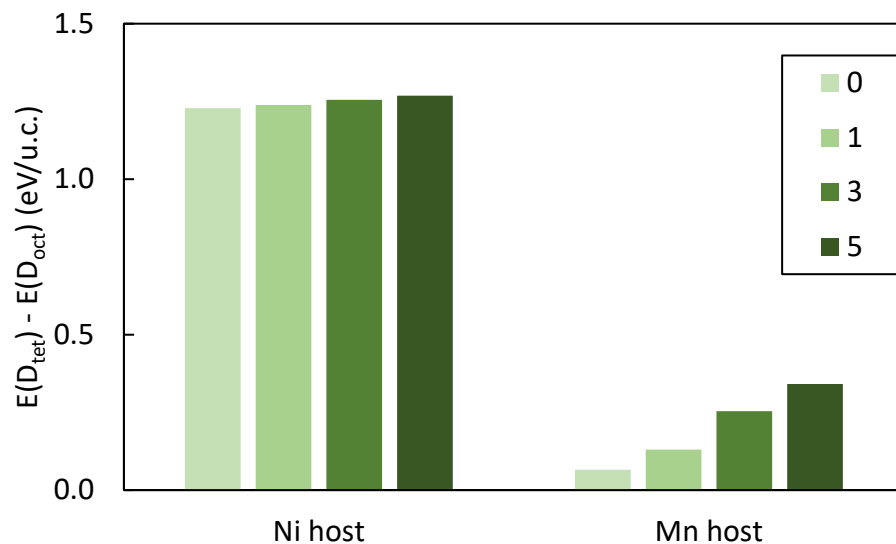


Figure S7. Energy difference between Li-Al D_{oct} and D_{tet} configurations (i.e. Li-Al dumbbell formation energy) in Ni and Mn hosts comparing effects of different values of the Hubbard U correction.

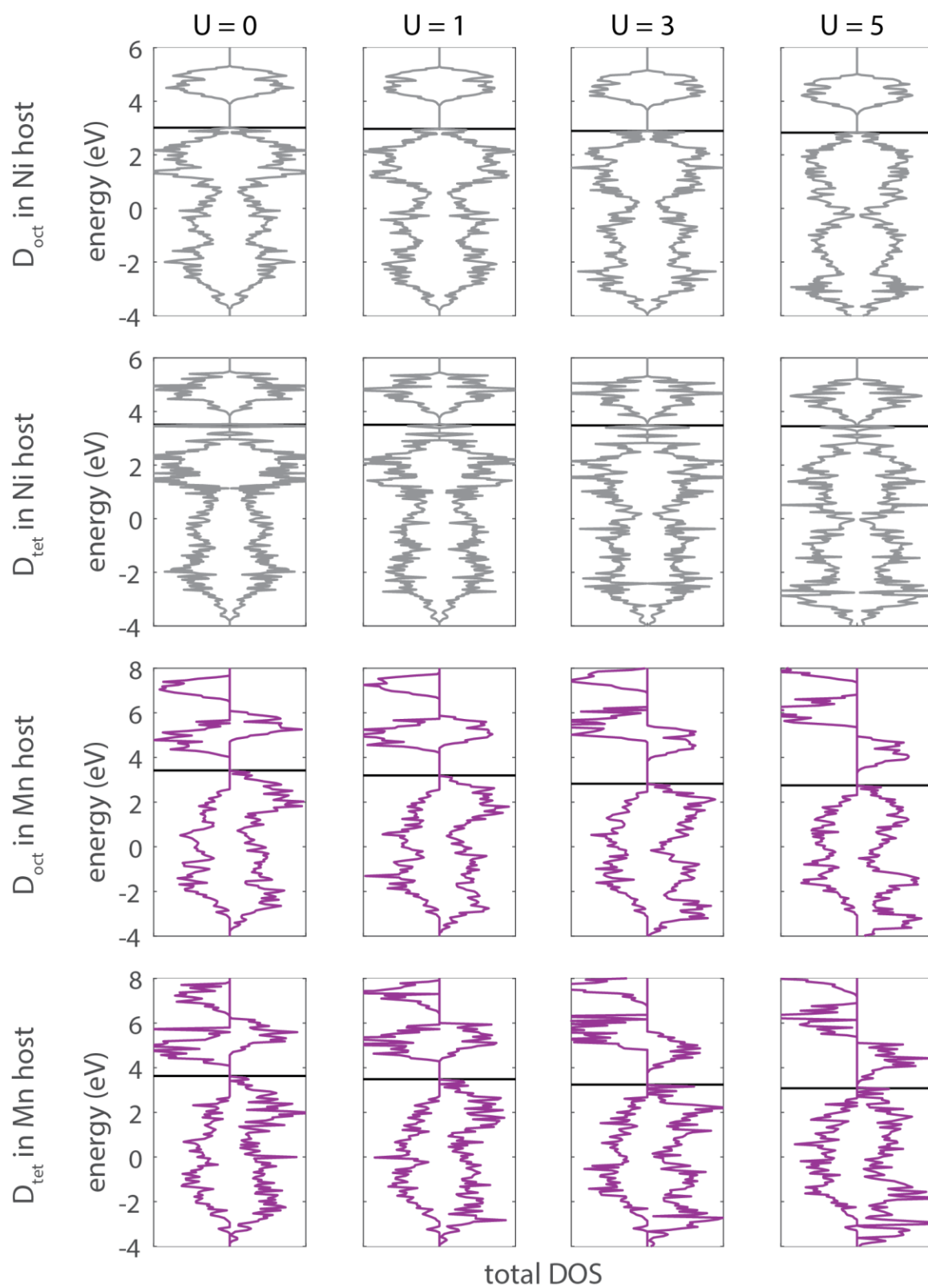


Figure S8. Total DOS for Li-Al D_{oct} and D_{tet} configurations in Ni and Mn hosts comparing effects of different values of the Hubbard U correction.

The total DOS plots of Figure S8 are qualitatively similar for the range of U values tested. Nevertheless, as the U value increases, the gap between t_{2g} and e_g states decreases. This has a very small effect on Li-Al dumbbell formation in the Ni host, as the energy changes by less than 50 meV/u.c. between the U = 0 and 5 eV values (Figure S7). The difference is more pronounced in the Mn host as dumbbell formation goes from 65 meV/u.c. without U correction to 342 meV/u.c. with a U = 5 eV correction. Since the shape of the total DOS and the relative energies between the hosts maintain the same trends for all values of U tested, we conclude that the general conclusions found in the manuscript are consistent for any reasonable value of the Hubbard U.

TM migration

We calculated the energy for moving an octahedral TM in the TM layer into an adjacent tetrahedral site in the Li layer for Ni in a Ni host, Co in a Ni host, Ni in a Co host, and Co in a Co host. Since there were no extra cations or background charge added to the system, all TM atoms are assumed to have a nominal 4+ charge. The lattice parameters and atom positions were allowed to fully relax. The k-point mesh density used was 30 \AA and the energy cutoff for these calculations was 520 eV. The energies of the tetrahedral TM relative to the octahedral TM are shown in Figure S9.

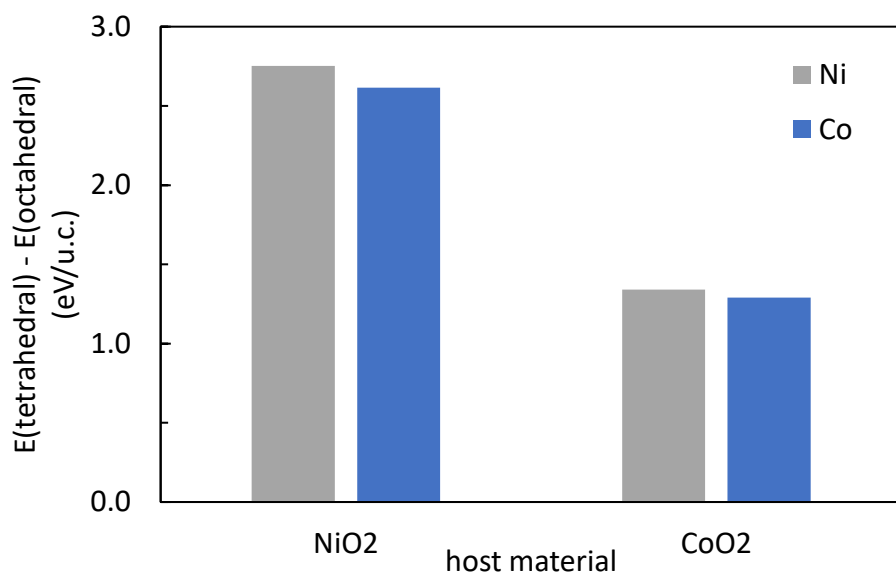


Figure S9. Energy for moving a TM atom from the TM layer into an adjacent tetrahedral site in the Li layer. The color corresponds to the host in which the migrating atom (Ni or Co) is moving. The host has a much stronger effect on the energy than does the identity of the migrating atom.

Energy cutoff and k-point convergence

Parameter convergence was performed for k-point mesh density and energy cutoff values. A range of k-point mesh density and energy cutoff values were tested for a Li-Al D_{tet} defect in Ni, Co, and Mn hosts. The results for k-point convergence are shown in Figure S10 and Table S1. Energy cutoff convergence is shown in Figure S11. The values used in relaxation calculations for this manuscript were at least 30 \AA for the k-point mesh density and 520 eV for the energy cutoff. These values meet convergence to about 1 meV/atom. The k-point mesh density for DOS calculations was 40 \AA .

Table S1. Densities and associated grids used for k-point convergence. Values given are k-point mesh density (\AA) and the resulting k-point grid from that density.

Ni host	Co host	Mn host
26 3x3x3	26 3x3x3	26 3x3x3
28 4x4x4	30 4x4x4	30 4x4x4
36 5x5x5	38 5x5x5	38 5x5x5
44 6x6x6	50 6x6x6	50 6x6x6
60 8x8x8	60 8x8x8	60 7x7x7

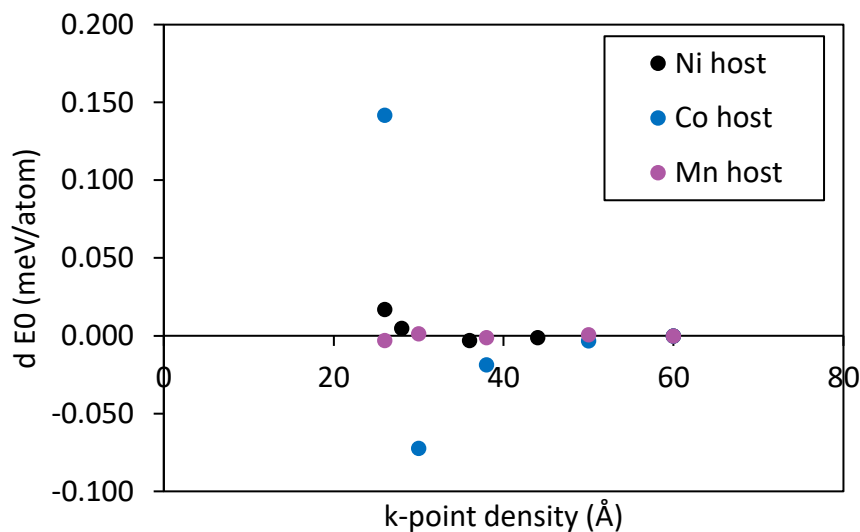


Figure S10. K-point convergence.

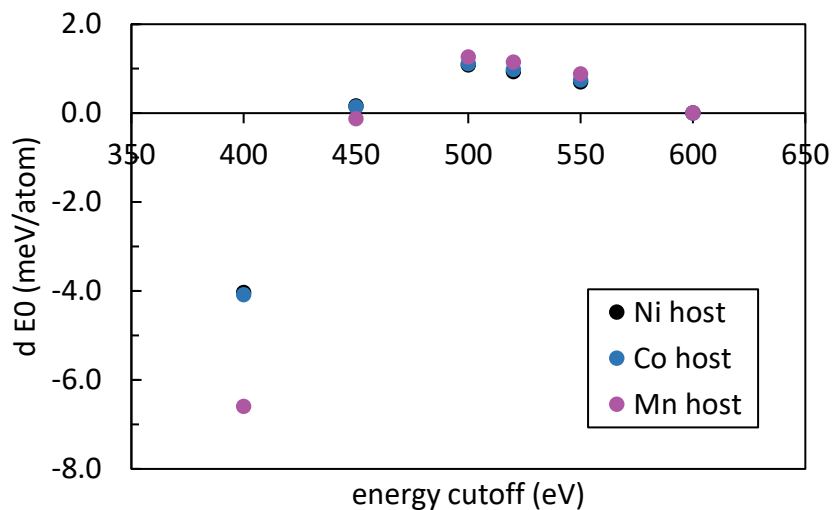


Figure S11. Energy cutoff convergence.

References

- ¹ Y. S. Meng, Y. Hinuma and G. Ceder, *J. Chem. Phys.*, 2008, **128**, 104708(1–8).
- ² E. B. Isaacs and C. A. Marianetti, *Phys. Rev. B*, 2017, **95**, 045141(1–18).